

Article

Not peer-reviewed version

---

# The Aggregation-Induced Emission Enhancement Properties of Heteroaryl Fused Triazapentalens Synthesis and Fluorescence Characteristics

---

[Yingchun Wang](#), [Junfeng Wu](#)<sup>\*</sup>, [Wim Dehaen](#)<sup>\*</sup>

Posted Date: 8 October 2024

doi: 10.20944/preprints202410.0543.v1

Keywords: triazapentalene; pyridine-fused triazapentalene; Suzuki cross-coupling; CH arylation; fluorescent properties; solid-state; aggregated state



Preprints.org is a free multidiscipline platform providing preprint service that is dedicated to making early versions of research outputs permanently available and citable. Preprints posted at Preprints.org appear in Web of Science, Crossref, Google Scholar, Scilit, Europe PMC.

Copyright: This is an open access article distributed under the Creative Commons Attribution License which permits unrestricted use, distribution, and reproduction in any medium, provided the original work is properly cited.

## Article

# The Aggregation-Induced Emission Enhancement Properties of Heteroaryl Fused Triazapentalenes: Synthesis and Fluorescence Characteristics

Yingchun Wang <sup>1,2</sup>, Junfeng Wu <sup>1,\*</sup> and Wim Dehaen <sup>2,\*</sup>

<sup>1</sup> Henan Key Laboratory of Water Pollution Control and Rehabilitation Technology, Henan University of Urban Construction, Pingdingshan 467036, PR China

<sup>2</sup> Sustainable Chemistry for Metals and Molecules, Department of Chemistry, KU Leuven, Celestijnenlaan 200F, 3001 Leuven, Belgium

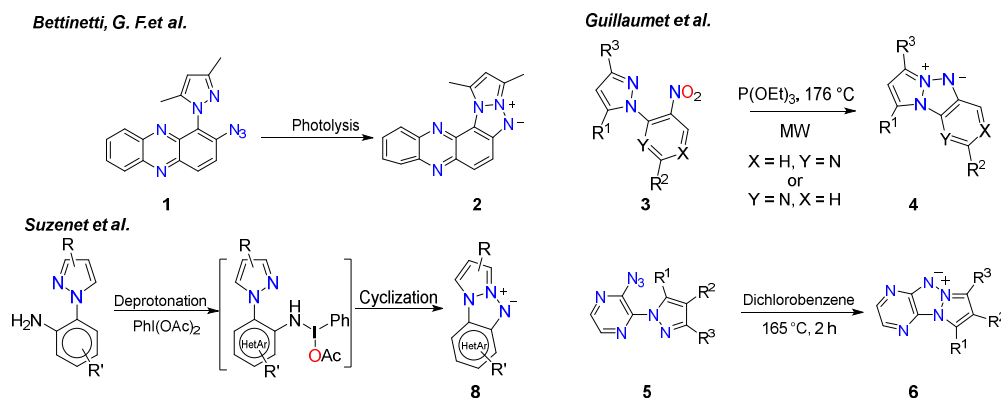
\* Correspondence: jf8047@163.com (J.W.); wim.dehaen@kuleuven.be (W.D.)

**Abstract:** A pyridine-fused triazapentalene shows weak fluorescence in solution, and is readily accessible via nitrene-mediated cyclization. In this research, a modified Cadogan reaction was used to synthesize **HetATAP1**. Palladium-catalyzed reactions have been demonstrated as post-functionalization methods. Interestingly, Suzuki cross-coupling with various boronic acids resulted in poor to moderate yields of the products **HetATAP2-5** arylated on the azole moiety. Direct CH arylation of **HetATAP1** gave the products with the same regiochemistry in satisfactory yields. The structures of **HetATAP2-5** were confirmed using NMR analysis. In addition, the fluorescence properties of **HetATAP2-5** were studied in the solid-state and solution at room temperature, and the photophysical properties of **HetATAP3** and **4** in the aggregated state were both measured in ACN/water and THF/water mixtures, respectively.

**Keywords:** triazapentalene; pyridine-fused triazapentalene; Suzuki cross-coupling; CH arylation; fluorescent properties; solid-state; aggregated state

## 1. Introduction

Heteroaryl-fused triazapentalenes (HetATAPs), more specifically *N*-heteroaryl triazapentalenes (*N*-HetATAPs), show fluorescent properties that are of interest for potential future applications [1–7]. Currently, only two mainly synthetic pathways toward HetATAPs have been reported [2,3,8–11], as shown in Scheme 1. The first published procedure mostly focus on the deoxygenation of 1-(*o*-nitro(hetero)aryl)pyrazoles and the thermolysis or photolysis of 1-(*o*-azido(hetero)aryl)pyrazoles [10,11]. In particular, **HetATAP** has been studied by the Bettinetti group, forming in unreactive media starting from 2-azido-1-(3,5-dimethylpyrazol-1-yl)phenazine **1**. The triazapentalene **2** was produced by intramolecular trapping of the formed nitrene. On the other hand, the synthetic methodology of Guillaumet et al. involves a deoxygenation reaction using nitro(pyrazolyl)pyridines **3**, which leads to pyridine-fused triazapentalenes **4** [3]. Although the deoxygenation reaction was only slightly influenced by the substituents of the pyrazole core, the modification of nitropyridine had a considerable impact on the reaction result. Later in 2009, the same group reported a library of pyrazine-fused triazapentalenes **6** by the thermolysis of 2-azido-3-(pyrazol-1-yl)pyrazines **5**, starting from nitropyrazoles and 2-azido-3-chloropyrazine [2]. The second reported pathway toward compound **8** begins with coupling reactions or nucleophilic aromatic substitutions with halogenated heterocyclic amines and pyrazole derivatives, followed by oxidative cyclization (Scheme 1, Suzenet et al.) [6,12]. Complementary to the radical reaction, under basic conditions in the presence of hypervalent iodine, the direct formation of intramolecular N-N bond takes place to form the desired **HetATAP** derivatives. Unfortunately, in function of the substitutions on the fused ring and the position of the amine, the reaction yields were variable.



**Scheme 1.** Synthetic pathways toward heteroaryl-fused triazapentalenes (HetATAPs) and the numbering of the triazapentalene core.

Applying the oxidative intramolecular N-N bond formation, Suzenet et al. studied the photophysical properties of HetATAP derivatives [6]. However, most of them exhibit modest to poor fluorescence quantum yields in solution. The variable quantum yields can be attributed to either the charge of the nitrogen atoms in the heteroaryl moiety or substituents on the azole moiety. Introducing two nitrogen atoms in the fused ring and/or an electron-withdrawing group on the azole ring in the case of R<sup>3</sup> position can improve the quantum yields of the resulting dyes in solution [6,7].

In 2001, Tang et al. reported that the aggregation of silole molecules induced light emission, which was opposite to the well-known aggregation-caused quenching (ACQ) [13]. Aggregation-induced emission enhancement (AIEE) has sparked considerable interest in its broad potential applications in physics [14], chemistry [15], biology [16–19], and material science [20–23]. However, as the formation of delocalized excitons or excimers may lead to enhanced non-radiative inactivation of the excited state, most organic molecules show fluorescence ACQ in their aggregated or solid state. The reported organic fluorescence dyes exhibit the AIEE characteristics, such as siloles [13,24–26], tetraphenylethylene (TPE) [27,28], 1-cyano-trans-1,2-bis(4'-methylbiphenyl)ethylene (CN-MBE) [29,30], 1,4-di[(E)-2-phenyl-1-propenyl]benzene (PPB) [31,32], and salicylaldehyde azine derivatives [33,34].

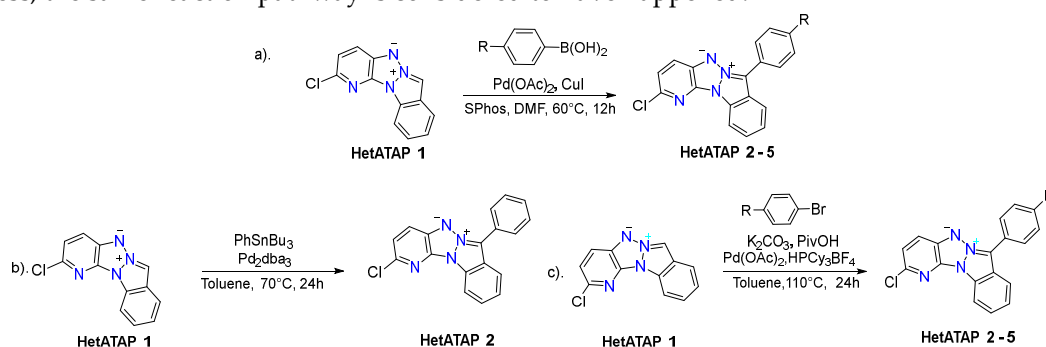
To date, the photophysical properties of HetATAP derivatives have only been reported in solution. The successful applications of HetATAPs are limited by their use as fluorescent probes in living cells and fluorescent dyes inserted into LDH host structures and polymers [1,5,7,35]. Because of the growing interest in HetATAP fluorophores, the initial goal of the present work was to expand the variety of substitution patterns on the heteroaryl moiety of triazapentalenes via post-functionalization strategies and study the photophysical properties of HetATAP in solids. For this purpose, the readily available Cadogan reaction was chosen as the synthetic pathway to obtain **HetATAP1**, and the feasibility of the palladium-catalyzed cross-coupling reactions was demonstrated. Herein, we describe the synthesis of HetATAP derivatives and their interesting solid-state fluorescent properties. To the best of our knowledge, the photophysical properties of solid-state HetATAPs have not been reported until now.[1]

## 2. Results and Discussion

### 2.1. Synthesis

To start our investigation, the desired **HetATAP1** was obtained using a modified Cadogan reaction (see SI Scheme S1) [3]. In an attempt to arylate heteroaryl-fused triazapentalene, procedures previously reported for the arylation of 1,3a,6a-triazapentalene with palladium catalysis were applied to **HetATAP1** [36]. The reported procedure with a Suzuki cross-coupling reaction was first carried out taking advantage of the presence of a chlorine atom on the pyridine moiety, and was performed with one equivalent of phenylboronic acid in the presence of CuI in DMF at 60 °C for 12 h. Surprisingly, a CH arylation occurred instead of the expected coupling reaction (Scheme 2a). The

unexpected compound **HetATAP2** was formed and confirmed via NMR analysis. In addition, we have sequentially attempted Stille coupling reaction with  $\text{PhSnBu}_3$  and direct palladium-catalyzed CH arylation with bromobenzene using toluene as solvent, which provided the same product (Scheme 2b and 2c). Similar reaction yields were obtained for **HetATAP2** from the Suzuki reaction and the direct CH arylation, but only 13% from the Stille coupling reaction. Hence, to extend the substituents, the Suzuki reaction and the direct CH arylation were carried out with different boronic acids and bromoarenes, respectively (Table 1). The reaction yields of the direct CH arylation were quite satisfying, and consequently higher than those of Suzuki reactions. In 2008, Gorelsky et al. reported the mechanism of the direct CH bond cleavage in the presence of  $\text{Pd}(\text{OAc})_2$  and potassium carbonate for the (electron-rich) heteroarenes [37]. As mentioned above, the direct palladium-catalyzed CH arylation conditions were adopted for the arylation of 1,3a,6a-triazapentalene, where arylation may occur via a concerted metalation-deprotonation in the presence of carbonate. For this process, the same reaction pathway is considered to have happened.



**Scheme 2.** The synthetic pathways towards HetATAPs 2–5. (a). Suzuki cross-coupling reaction, (b). Stille coupling reaction, (c) Direct palladium-catalysed CH arylation.

**Table 1.** The reaction yields of various pathways towards **HetATAPs 2–5**.

HetATAP	R	Yield (%)		
		a	b	c
2	H	53	13	66
3	OMe	47	– <sup>a</sup>	62
4	COOEt	35	– <sup>a</sup>	51
5	N(Me) <sub>2</sub>	30	– <sup>a</sup>	73

<sup>a</sup> Reaction was not carried out. <sup>b</sup> Experimental conditions: Suzuki cross-coupling reaction: HetATAPs (0.2 mmol, 1 equiv), boronic acids (0.24 mmol, 1.2 equiv),  $\text{Pd}(\text{OAc})_2$  (27 mg, 0.12 mmol, 0.6 equiv), CuI (15.2 mg, 0.08 mmol, 0.4 equiv), SPhos (10 mg, 0.023, 0.12 equiv) and DMF (2 mL), 12 h; Stille reaction: HetATAP1 (24.3 mg, 0.1 mmol, 1 equiv),  $\text{PhSnBu}_3$  (44.2 mg, 0.12 mmol, 1.2 equiv),  $\text{Pd}_2\text{dba}_3$  (5 mg, 0.005, 0.05 equiv), 24 h; (3). Palladium-catalyzed CH arylations: HetATAP1 (0.2 mmol, 1 equiv), bromoarene reagents (0.2 mmol, 1.0 equiv),  $\text{Pd}(\text{OAc})_2$  (2.4 mg, 0.01 mmol, 0.05 equiv),  $\text{Cy}_3\text{HBF}_4$  (7.8 mg, 0.02 mmol, 0.1 equiv), pivalic acid (6.6 mg, 0.03, 0.3 equiv),  $\text{K}_2\text{CO}_3$  (88 mg, 0.6 mmol, 3.0 equiv) and dry toluene (4 mL), 24 h.

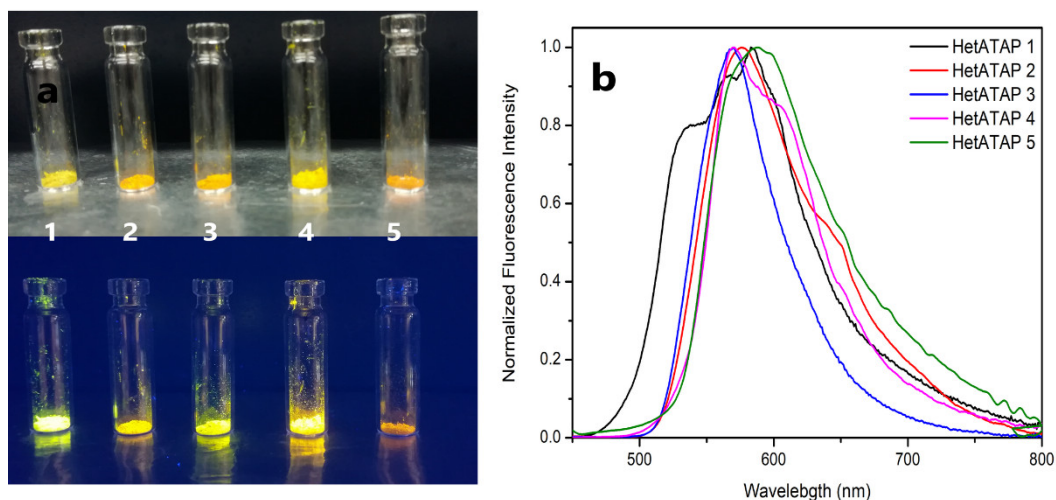
## 2.2. Photophysical Measurements

### 2.2.1. Fluorescence in the Solid-State

The absorption and emission spectra were taken for **HetATAP1** and its postmodified products **HETATAP2–5** in solid-state at room temperature. The color of these compounds under the naked eye and a UV lamp are collected in Figure 1a, and the emission spectra for **HetATAP1–5** are shown in Figure 1b. The photophysical parameters are listed in Table 2. The color of all the compounds is slightly different. Observing the brightness of all compounds under UV light, **HetATAP2 and 5** are less intense compared to **HetATAP1**, while **HetATAP3 and 4** are slightly more intense, suggesting the difference of quantum yields of fluorescence ( $\Phi_F$ ). Compared to the precursor **HetATAP1**, the absorption spectra of **HetATAP 2–4** are redshifted and the emission spectra are slightly blueshifted, except for **HetATAP5**. The presence of additional functional groups which could disturb the

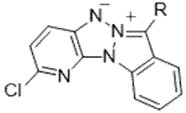


molecular planarity of **HetATAP1** might be responsible. In **HetATAP 2-5**, the Stokes shift is smaller than that of **HetATAP1**, suggesting more coplanarity. Since **HetATAP3** and **4** have good fluorescent properties, it is of utmost interest to study them further.



**Figure 1.** The color of compounds under naked eyes and UV lamp (a) (365 nm) and normalized, fluorescence emission spectra of **HetATAPs 1-5** in the solid-state (b).

**Table 2.** Fluorescence properties of **HetATAP1-5** in solid state.

	$\lambda_{\text{abs, max}}$ (nm)	$\lambda_{\text{em, max}}$ (nm)	Stokes Shift ( $\text{cm}^{-1}$ )	$\Phi_F$ (%)
HetATAP1	460	584	4600 $\pm$ 50	10
HetATAP2	525	576	1680 $\pm$ 50	5
HetATAP3	520	570	1680 $\pm$ 50	12
HetATAP4	520	571	1710 $\pm$ 50	20
HetATAP5	485	588	3610 $\pm$ 50	5

### 2.2.2. Fluorescence in Solution

For the **HetATAPs 2-5** dyes in DCM at room temperature, absorption spectra show the bathochromically shifted spectra compared to **HetATAP1**. The phenyl and 4-methoxyphenyl substituents in **HetATAPs 2** and **3** gave an approximately 30 nm bathochromic shift, whereas the 4-ethoxycarbonylphenyl and 4-dimethylaminophenyl substituents showed a shift of around 43 nm (Figure 2). As mentioned earlier, these dyes show very weak emission properties in solution, suggesting the substituents at  $R^3$  are not helpful for their fluorescence quantum yields, which is the same as the reports for pyrazine-fused triazapentalenes [6,7].

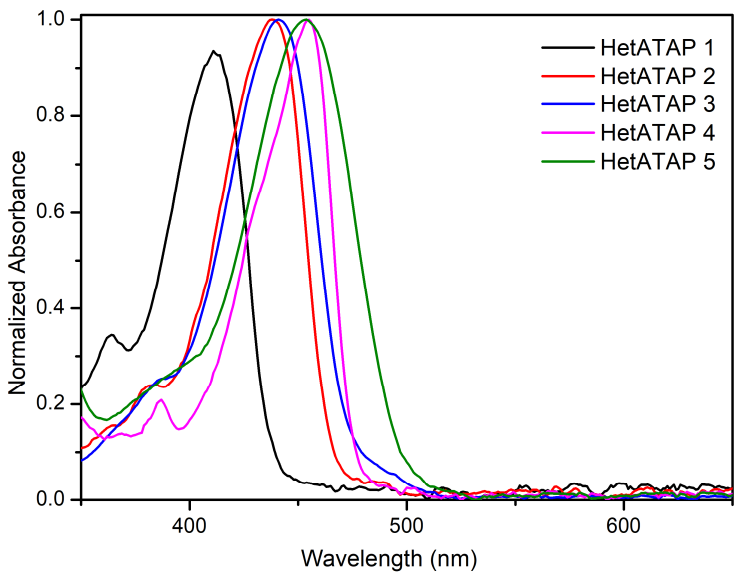


**Figure 2.** Normalized, absorption spectra of HetATAPs **1** and **2–5** in the DCM.

The different solvent effect on the photophysical parameters of **HetATAP3** and **4** in solution at room temperature were investigated (Figure 3, Table 3). The maximum absorption wavelength ( $\lambda_{\text{abs, max}}$ ) of these compounds were barely affected by the polarity of the solvent, indicating that in the ground state and excited state, their dipole moments are almost equal (Figure 3a, 3b). However, the effect of solvent polarity on the molar absorption coefficients ( $\epsilon$ ) was more apparent (Table 3). The  $\epsilon$  values of **HetATAP3** and **4** in DCM and THF were much higher than that in other solvents, respectively. In addition, the molar absorption coefficients of **HetATAP3** and **4** underwent only a small change in other solvents, except that **HetATAP3** gave a higher  $\epsilon$  value in ACN. Notably, the solubility of **HetATAP4** in ACN is too poor to check the  $\epsilon$  value. The fluorescence quantum yields ( $\Phi_F$ ) of **HetATAP1** and **2–5** are less than 0.01 in organic solvents, so these compounds show almost no fluorescence in solution.

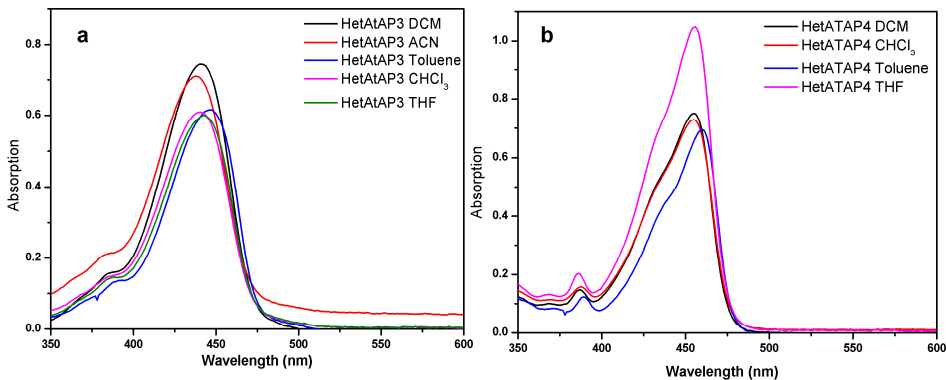


**Figure 3.** Absorption spectra of compounds **HetATAP3** (a) and **4** (b) in different solution (200  $\mu\text{M}$ ).

**Table 3.** Optical data measured in different solutions.

Dye	Matrix	$\lambda_{\text{abs, max}}$ (nm)	$\epsilon(\text{dm}^3 \text{ mol}^{-1} \text{ cm}^{-1})$	$\lambda_{\text{em, max}}$ (nm)
HetATAP3	DCM	441	39, 194	604
	$\text{CHCl}_3$	440	30, 454	610
	ACN	438	35, 482	606
	Toluene	447	30, 799	610
	THF	443	29, 989	614

Dye	Matrix	$\lambda_{\text{abs, max}}$ (nm)	$\epsilon(\text{dm}^3 \text{ mol}^{-1} \text{ cm}^{-1})$	$\lambda_{\text{em, max}}$ (nm)
HetATAP4	Solid			570
	DCM	455	37,524	616
	$\text{CHCl}_3$	455	36,420	622
	Toluene	460	34,741	606
	THF	456	52,373	642
	Solid			571

### 2.3. Fluorescence in the Aggregated State

The AIEE properties of compounds **HetATAP3** and **HetATAP4** were investigated in a mixture of ACN/THF and water (Figure 4). In organic solvents, **HetATAP3** and **HetATAP4** are well dispersed and show absorption and weak emission spectra. However, the situation was reversed when they were placed in a solvent-poor system under the same conditions. The weak absorption and strong fluorescence emission indicate that they formed aggregated states and the aggregation-induced fluorescence emission. In addition, in the solvent-poor system, the maximum absorption wavelengths of **HetATAP3** and **HetATAP4** showed a significant blue shift of 20 nm and 30 nm, respectively.

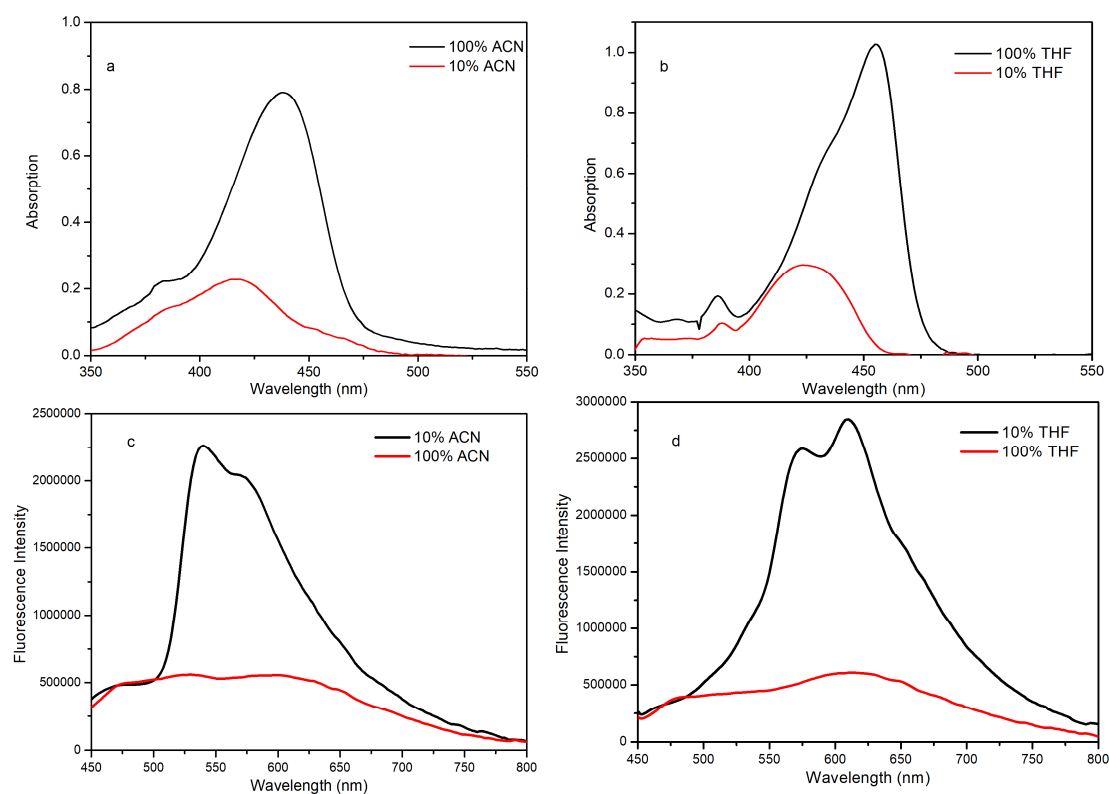


**Figure 4.** Absorption (a) and fluorescence emission spectra (c) of **HetATAP3** ( $\lambda_{\text{ex}} = 438$  nm) (200  $\mu\text{M}$ ) in ACN solution and “aggregate” (ACN/water, 1:9, v/v); absorption (b) and fluorescence emission spectra (d) of **HetATAP4** ( $\lambda_{\text{ex}} = 450$  nm) (200  $\mu\text{M}$ ) in THF solution and “aggregate” (THF/water, 1:9, v/v).

To further investigate the AIEE properties of **HetATAP3** and **HetATAP4**, UV-Vis absorption and fluorescence emission spectra were measured in different volume fractions of ACN/THF and water mixtures (Figure 5 and 6). Compared to the UV-Vis absorption spectra of compounds **HetATAP3** and **HetATAP4** at different test times (10 min, 3.0 h, 24 h), the maximum absorption wavelengths remained almost unchanged when the organic fraction was between 40% and 100% (Figure 5a-c and 6a-c). However, there was a gradual decrease in the intensity of absorption, especially for compound **HetATAP3**. When the organic fraction was reduced from 40% to 30%, the

intensity of absorption decreased rapidly and there was a significant blue shift in the maximum absorption wavelength. When the duration of the test was increased from 3 to 24 hours, the absorption intensity decreased sharply when the system contained 40% organic solvent. The Mie scattering caused by nanoparticles may be responsible for the decreased intensity [38–40].

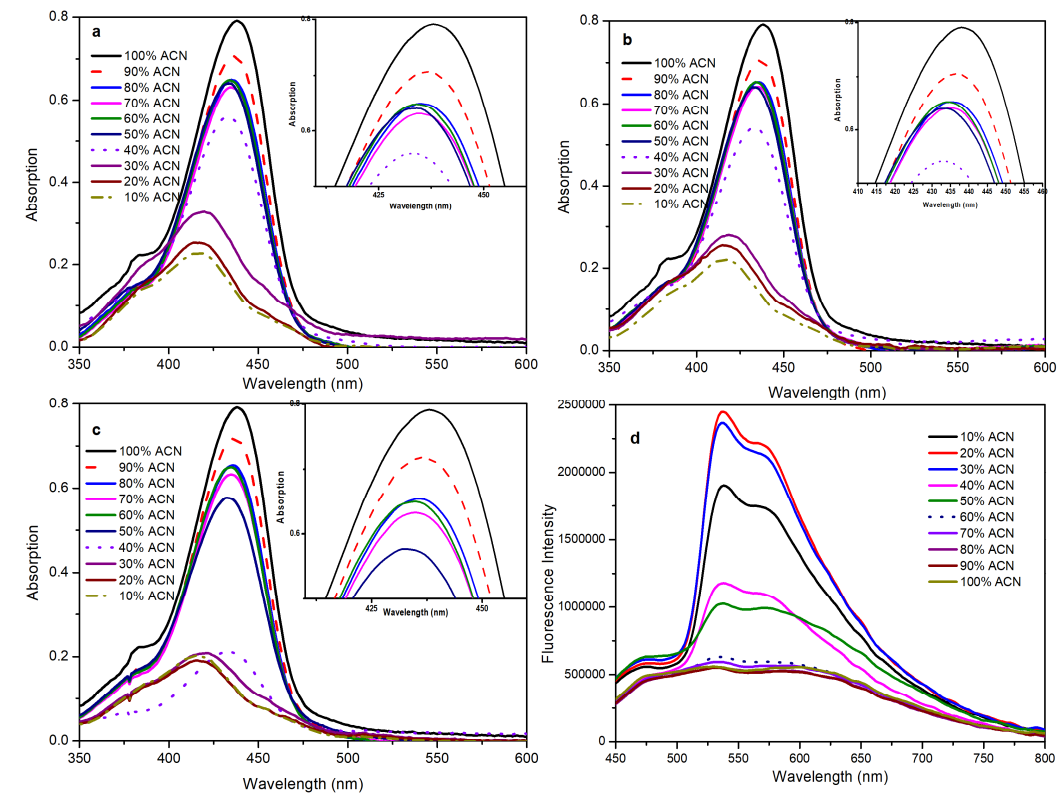


**Figure 5.** Absorption (a, b, c) of compound **HetATAP3** (200 μM) with different duration for (10 min, 3 h, 24 h) and fluorescence spectra (d) with duration over 24 hours in ACN/water mixtures with different ACN contents.

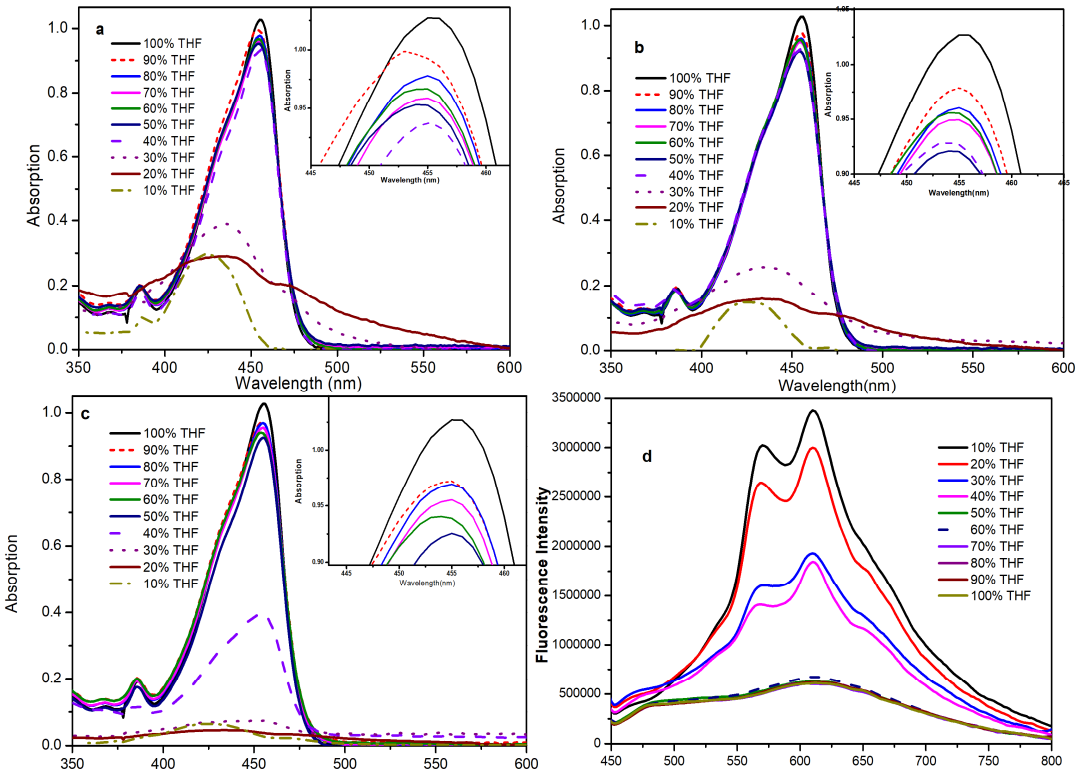




**Figure 6.** Absorption (a, b, c) of compound **HetATAP4** (200  $\mu$ M) with different duration for (10 minutes, 3.0 h, 24 h) and fluorescence spectra (d) with duration over 24 hours in THF/water mixtures with different THF contents.

The **HetATAP3** and **HetATAP4** derivatives (Figure 5d and Figure 6d) showed very weak fluorescence emission in dilute organic solvent over 24 hours. Reducing the organic solvent content in the solution containing the compound **HetATAP4** to 60% (v/v), or even to 50%, the fluorescence properties were barely changed as the compound could be well dissolved into the solvent system. However, as the organic solvent content in the solution system dropped from 50% to 0, the fluorescence emission intensity gradually increased (Figure 5d and Figure 6d), while the absorption intensity decreased sharply (Figure 5c and Figure 6c). Furthermore, the maximum emission wavelength of **HetATAP3** and **HetATAP4** started to split into two clear peaks with a significant blue shift of 80 nm and 30 nm, respectively. Due to the poor solubility of the compounds in water, they may have aggregated in the solvent systems with lower organic solvent contents (40%-10%, v/v). Therefore, **HetATAP3** and **HetATAP4** are AIEE active. The effect of the volume fraction of water on the AIEE phenomenon and the color changed was observed under a UV lamp (365 nm) (Figure 7).

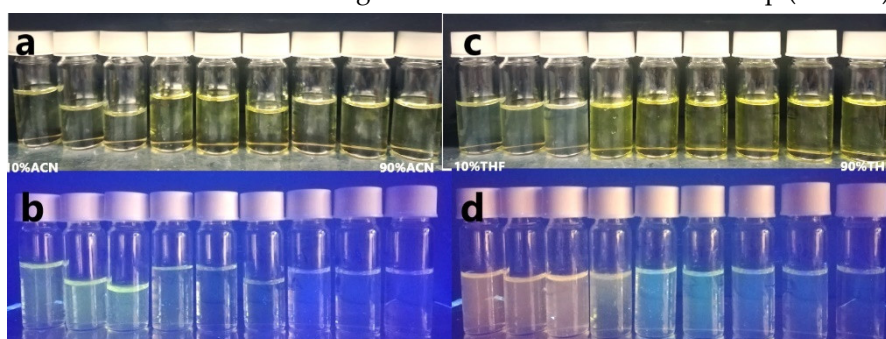


**Figure 7.** The color of compound **HetATAP3** in ACN/water with different ACN contents under the naked eye (a) and under the UV lamp (365 nm) (b). The color of compound **HetATAP4** in THF/water with different THF contents under naked eye (c) and under the UV lamp (365 nm) (d).

To further investigate the AIEE phenomenon, the fluorescence intensities of compounds **HetATAP3** and **HetATAP4** were studied for different durations in ACN/water and THF/water mixtures with an organic solvent content of 10% v/v, respectively (Figure 8). The fluorescence intensities were measured immediately after shaking the freshly prepared solutions by hand. The results showed the fluorescence of compounds **HetATAP3** and **HetATAP4** increased and almost reached its maximum value within 30 and 10 min, respectively. It was assumed that the initial shaking increases the chances of some of the dye molecules gathering together to form tiny particles, and then the remaining molecules gradually associate to the particles formed (see SI Figure S12). After a certain amount of time, the compounds precipitated completely from the solution, and the enhancement of fluorescence intensity ceased.

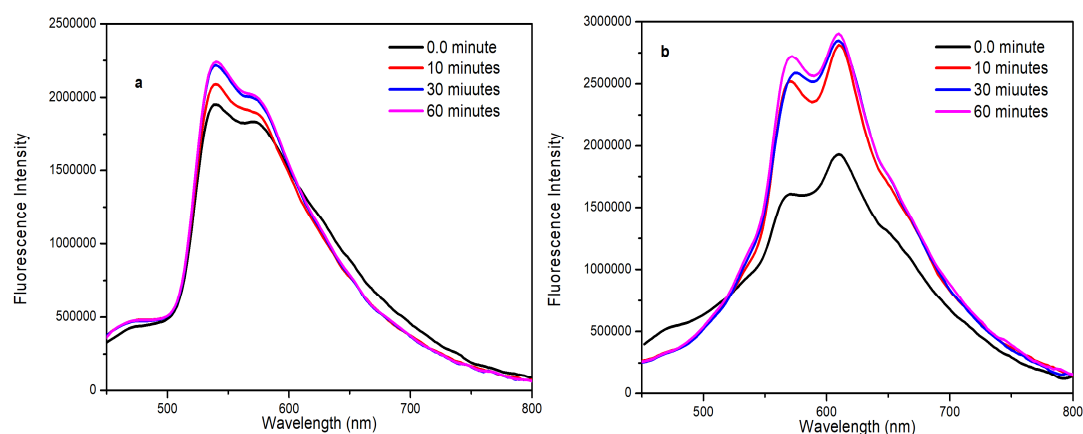


**Figure 8.** Dependence of the fluorescence intensity of compounds **HetATAP3** (a) and **HetATAP4** (b) (200  $\mu$ M) to aggregating time in ACN/water and THF/water (1:9, v/v), respectively.

### 3. Materials and Methods

#### 3.1. Chemical and Materials

All chemicals were purchased from Acros Organics, Merck, J&K Scientific, Fluorochem and TCI Europe and used as received. Solvents were dried prior to use. For column chromatography, 70–230 mesh silica gel 60 (Acros) was used as the stationary phase.

#### 3.2. Instrumentation

$^1\text{H}$  and  $^{13}\text{C}$  NMR spectra were recorded on a Bruker Avance 300, Bruker Avance III HD 400 or a Bruker Avance II<sup>+</sup> 600 spectrometer. Chemical shifts ( $\delta$ ) are reported in parts per million (ppm) referenced to tetramethylsilane (0.00 ppm) as an internal standard for samples in  $\text{CDCl}_3$ , or to the respective solvent for samples in  $\text{DMSO-d}_6$  (2.50 ppm).  $^{13}\text{C}$  NMR spectra were referenced to the respective solvent signals ( $\text{CDCl}_3$ , 77.16 ppm). High-resolution mass spectra were acquired on a quadrupole orthogonal acceleration time-of-flight mass spectrometer (Synapt G2 HDMS, Waters, Milford, MA). Melting points (not corrected) were determined using a Reichert Thermovar apparatus.

UV-Vis absorption spectra were recorded on a PerkinElmer Lambda 950 spectrophotometer using blank correction. Fluorescence spectra and excitation spectra were recorded on a HORIBA Jobin Yvon Fluorolog FL3-22 fluorimeter and corrections for the excitation beam intensity, the wavelength dependent sensitivity of the detector and the optical path were applied.

#### 3.3. Synthesis

##### 3.3.1. General Procedure for Suzuki Cross-Coupling Reaction

To an oven-dried reaction tube equipped with a magnetic stirring bar were added HetATAPs (0.2 mmol, 1 equiv), boronic acids (0.24 mmol, 1.2 equiv),  $\text{Pd}(\text{OAc})_2$  (27 mg, 0.12 mmol, 0.6 equiv),  $\text{CuI}$  (15.2 mg, 0.08 mmol, 0.4 equiv), SPhos (10 mg, 0.023, 0.12 equiv) and DMF (2 mL). The mixture was left and stirred for 12 hours at 60  $^\circ\text{C}$  in an aluminum heating block. The crude reaction mixture was dissolved in ethyl acetate (20 mL) and washed with water ( $2 \times 20$  mL) and brine ( $1 \times 20$  mL). The organic layer was subsequently dried over magnesium sulfate and concentrated under reduced pressure. Further purification by column chromatography, using a PE-DCM gradient as the eluent, afforded the solid compounds.

##### 3.3.2. Stille Coupling Reaction of Compound HetATAP1

HetATAP1 (24.3 mg, 0.1 mmol, 1 equiv),  $\text{PhSnBu}_3$  (44.2 mg, 0.12 mmol, 1.2 equiv) and  $\text{Pd}_2\text{dba}_3$  (5 mg, 0.005, 0.05 equiv) were added to an oven-dried reaction tube equipped with a magnetic stirring bar and dissolved in toluene (1 mL) under a nitrogen atmosphere. The reaction mixture was left and stirred at 70 $^\circ\text{C}$  for 24 hours. The reaction mixture was diluted with EtOAc (20 mL) and washed with water ( $2 \times 20$  mL) and brine ( $1 \times 20$  mL). The organic layer was subsequently dried over magnesium sulfate and concentrated under reduced pressure. Further purification by column chromatography, using a PE-DCM ((1:1–0:1)) gradient as the eluent, afforded a yellow solid HetATAP2 (4 mg, 13%).

##### 3.3.3. General Procedure for Palladium-Catalyzed CH Arylation

To an oven-dried reaction tube equipped with a magnetic stirring bar were added HetATAP1 (0.2 mmol, 1 equiv), bromoarene reagents (0.2 mmol, 1.0 equiv),  $\text{Pd}(\text{OAc})_2$  (2.4 mg, 0.01 mmol, 0.05 equiv),  $\text{Cy}_3\text{HBF}_4$  (7.8 mg, 0.02 mmol, 0.1 equiv), pivalic acid (6.6 mg, 0.03, 0.3 equiv),  $\text{K}_2\text{CO}_3$  (88 mg, 0.6 mmol, 3.0 equiv) and dry toluene (4 mL). The mixture was left and stirred for 24 hours at 110  $^\circ\text{C}$  in an aluminum heating block. The reaction mixture was dissolved in ethyl acetate (20 mL) and washed with water ( $2 \times 20$  mL) and brine ( $1 \times 20$  mL). The organic layer was subsequently dried over

magnesium sulfate and concentrated under reduced pressure. Further purification by column chromatography, using a PE-DCM gradient as the eluent, afforded the solid compounds.

### 3.3.4. Experimental Details and Characterization Data

**HetATAP1:** Yellow solid. Yield 89.5 mg, 74%. Mp 192–195°C.  $^1\text{H}$  NMR (400 MHz,  $\text{CDCl}_3$ )  $\delta$  8.35 (d,  $J$  = 5.5 Hz, 1H), 7.98 (s, 1H), 7.80–7.73 (m, 1H), 7.67 (d,  $J$  = 8.5 Hz, 1H), 7.48 (d,  $J$  = 7.0 Hz, 2H), 7.33 (d,  $J$  = 8.5 Hz, 1H).  $^{13}\text{C}$  NMR (101 MHz,  $\text{CDCl}_3$ )  $\delta$  138.77, 138.40, 135.91, 125.03, 124.57, 123.66, 123.55, 121.16, 120.60, 118.70, 111.37, 98.33. HRMS (ESI-Q-TOF):  $m/z$   $[\text{M}+\text{H}]^+$  calcd for  $\text{C}_{12}\text{H}_7\text{ClN}_4$ : 243.0432, found: 243.0431.

**HetATAP2:** (1) Prepared following the general procedure for Suzuki cross-coupling reaction: **HetATAPs** (0.2 mmol, 1 equiv), phenylboronic acid (0.24 mmol, 1.2 equiv),  $\text{Pd}(\text{OAc})_2$  (27 mg, 0.12 mmol, 0.6 equiv),  $\text{CuI}$  (15.2 mg, 0.08 mmol, 0.4 equiv),  $\text{SPhos}$  (10 mg, 0.023, 0.12 equiv) and DMF (2 mL), 12 h. Purification by column chromatography, using a PE-DCM gradient (1:1–0:1) as the eluent, afforded **HetATAP2** (38 mg, 53%) as a yellow solid. (2). Prepared following the procedure for Stille coupling reaction: **HetATAP1** (24.3 mg, 0.1 mmol, 1 equiv),  $\text{PhSnBu}_3$  (44.2 mg, 0.12 mmol, 1.2 equiv),  $\text{Pd}_2\text{dba}_3$  (5 mg, 0.005, 0.05 equiv), 24 h. Purification by column chromatography, using a PE-DCM gradient (1:1–0:1) as the eluent afforded **HetATAP2** (4 mg, 13%). (3). Prepared following the general procedure for palladium-catalyzed CH arylations: **HetATAP1** (0.2 mmol, 1 equiv), bromobenzene (0.2 mmol, 1.0 equiv),  $\text{Pd}(\text{OAc})_2$  (2.4 mg, 0.01 mmol, 0.05 equiv),  $\text{Cy}_3\text{HBF}_4$  (7.8 mg, 0.02 mmol, 0.1 equiv), pivalic acid (6.6 mg, 0.03, 0.3 equiv),  $\text{K}_2\text{CO}_3$  (88 mg, 0.6 mmol, 3.0 equiv) and dry toluene (4 mL), 24 h. Purification by column chromatography, using a PE-DCM (1:1–0:1) gradient as the eluent, afforded the solid compounds **HetATAP2** (42 mg, 66%) as a yellow solid. Mp 192–194 °C.  $^1\text{H}$  NMR (400 MHz,  $\text{CDCl}_3$ )  $\delta$  8.52–8.40 (m, 1H), 8.35 (dd,  $J$  = 8.5, 1.2 Hz, 2H), 8.22–8.09 (m, 1H), 7.75 (d,  $J$  = 8.5 Hz, 1H), 7.67–7.59 (m, 2H), 7.61–7.52 (m, 2H), 7.48–7.38 (m, 1H), 7.35 (d,  $J$  = 8.5 Hz, 1H).  $^{13}\text{C}$  NMR (101 MHz,  $\text{CDCl}_3$ )  $\delta$  138.90, 138.71, 129.12, 128.14, 127.88, 126.57, 125.28, 124.00, 123.90, 123.02, 121.22, 120.83, 119.15, 111.53. HRMS (ESI-Q-TOF):  $m/z$   $[\text{M}+\text{H}]^+$  calcd for  $\text{C}_{18}\text{H}_{11}\text{ClN}_4$ : 319.0744, found: 319.0741.

**HetATAP3:** (1). Prepared following the general procedure for Suzuki cross-coupling reaction: **HetATAP1** (0.2 mmol, 1 equiv), 4-methoxyphenylboronic acid (0.24 mmol, 1.2 equiv),  $\text{Pd}(\text{OAc})_2$  (27 mg, 0.12 mmol, 0.6 equiv),  $\text{CuI}$  (15.2 mg, 0.08 mmol, 0.4 equiv),  $\text{SPhos}$  (10 mg, 0.023, 0.12 equiv) and DMF (2 mL), 12 h. Purification by column chromatography, using a PE-DCM gradient (1:1–0:1) as the eluent, afforded **HetATAP3** (32.9 mg, 47%) as a yellow solid. (2). Prepared following the general procedure for palladium-catalyzed CH arylations: **HetATAP1** (0.2 mmol, 1 equiv), 4-bromoanisole (0.2 mmol, 1.0 equiv),  $\text{Pd}(\text{OAc})_2$  (2.4 mg, 0.01 mmol, 0.05 equiv),  $\text{Cy}_3\text{HBF}_4$  (7.8 mg, 0.02 mmol, 0.1 equiv), pivalic acid (6.6 mg, 0.03, 0.3 equiv),  $\text{K}_2\text{CO}_3$  (88 mg, 0.6 mmol, 3.0 equiv) and dry toluene (4 mL), 24 h. Purification by column chromatography, using a PE-DCM (1:1–0:1) gradient as the eluent, afforded the solid compounds **HetATAP3** (43.4 mg, 62%) as a yellow solid. Mp 248–250°C.  $^1\text{H}$  NMR (400 MHz,  $\text{CDCl}_3$ )  $\delta$  8.45–8.35 (m, 1H), 8.26 (d,  $J$  = 8.9 Hz, 1H), 8.11–8.06 (m, 1H), 7.69 (d,  $J$  = 8.5 Hz, 1H), 7.57–7.48 (m, 1H), 7.31 (d,  $J$  = 8.5 Hz, 1H), 7.15 (d,  $J$  = 8.9 Hz, 1H).  $^{13}\text{C}$  NMR (101 MHz,  $\text{CDCl}_3$ )  $\delta$  159.28, 138.93, 138.37, 136.12, 129.97, 128.19, 125.05, 123.93, 122.88, 121.04, 120.61, 120.33, 119.11, 114.65, 111.49, 110.98, 55.45. HRMS (ESI-Q-TOF):  $m/z$   $[\text{M}]$  calcd for  $\text{C}_{19}\text{H}_{13}\text{ClN}_4\text{O}$ : 348.0778, found: 348.0778.

**HetATAP4:** (1). Prepared following the general procedure for Suzuki cross-coupling reaction: **HetATAP1** (0.2 mmol, 1 equiv), 4-ethoxycarbonylphenylboronic acid (0.24 mmol, 1.2 equiv),  $\text{Pd}(\text{OAc})_2$  (27 mg, 0.12 mmol, 0.6 equiv),  $\text{CuI}$  (15.2 mg, 0.08 mmol, 0.4 equiv),  $\text{SPhos}$  (10 mg, 0.023, 0.12 equiv) and DMF (2 mL), 12 h. Purification by column chromatography, using a PE-DCM gradient (1:1–0:1) as the eluent, afforded **HetATAP4** (27.3 mg, 35%) as a yellow solid. (2). Prepared following the general procedure for palladium-catalyzed CH arylations: **HetATAP1** (0.2 mmol, 1 equiv), ethyl 4-bromobenzoate (0.2 mmol, 1.0 equiv),  $\text{Pd}(\text{OAc})_2$  (2.4 mg, 0.01 mmol, 0.05 equiv),  $\text{Cy}_3\text{HBF}_4$  (7.8 mg, 0.02 mmol, 0.1 equiv), pivalic acid (6.6 mg, 0.03, 0.3 equiv),  $\text{K}_2\text{CO}_3$  (88 mg, 0.6 mmol, 3.0 equiv) and dry toluene (4 mL), 24 h. Purification by column chromatography, using a PE-DCM (1:1–0:1) gradient as the eluent, afforded the solid compounds **HetATAP4** (39.8 mg, 51%) as a yellow solid. Mp 249–251°C.  $^1\text{H}$  NMR (400 MHz,  $\text{CDCl}_3$ )  $\delta$  8.53–8.48 (m, 2H), 8.48–8.43 (m, 1H), 8.29–8.24 (m, 3H), 8.24–8.15

(m, 1H), 7.88 (dd,  $J = 8.2, 1.3$  Hz, 1H), 7.64–7.48 (m, 2H), 7.39 (dd,  $J = 8.2, 4.8$  Hz, 1H), 4.44 (q,  $J = 7.1$  Hz, 2H), 1.45 (t,  $J = 7.1$  Hz, 3H).  $^{13}\text{C}$  NMR (101 MHz,  $\text{CDCl}_3$ )  $\delta$  166.23, 139.56, 139.37, 137.33, 132.86, 130.24, 128.54, 125.55, 125.39, 124.20, 123.92, 123.09, 121.26, 119.58, 119.00, 111.41, 109.35, 61.04, 14.41. HRMS (ESI-Q-TOF):  $m/z$   $[\text{M}+\text{H}]^+$  calcd for  $\text{C}_{21}\text{H}_{15}\text{ClN}_4\text{O}_2$ : 391.0956, found: 391.0954.

**HetATAP5:** (1). Prepared following the general procedure for Suzuki cross-coupling reaction: **HetATAP1** (0.2 mmol, 1 equiv), 4-(dimethylamino)phenylboronic acid (0.24 mmol, 1.2 equiv),  $\text{Pd}(\text{OAc})_2$  (27 mg, 0.12 mmol, 0.6 equiv),  $\text{CuI}$  (15.2 mg, 0.08 mmol, 0.4 equiv),  $\text{SPhos}$  (10 mg, 0.023, 0.12 equiv) and DMF (2 mL), 12 h. Purification by column chromatography, using a PE-DCM gradient (1:1–0:1) as the eluent, afforded **HetATAP5** (22.1 mg, 30%) as a yellow solid. (2). Prepared following the general procedure for palladium-catalyzed CH arylations: **HetATAP1** (0.2 mmol, 1 equiv), 1-bromo-4-(dimethylamino)benzene (0.2 mmol, 1.0 equiv),  $\text{Pd}(\text{OAc})_2$  (2.4 mg, 0.01 mmol, 0.05 equiv),  $\text{Cy}_3\text{HBF}_4$  (7.8 mg, 0.02 mmol, 0.1 equiv), pivalic acid (6.6 mg, 0.03, 0.3 equiv),  $\text{K}_2\text{CO}_3$  (88 mg, 0.6 mmol, 3.0 equiv) and dry toluene (4 mL), 24 h. Purification by column chromatography, using a PE-DCM (1:1–0:1) gradient as the eluent, afforded the solid compounds **HetATAP5** (53.8 mg, 73%) as an orange-yellow solid. Mp 115–117 °C.  $^1\text{H}$  NMR (300 MHz,  $\text{CDCl}_3$ )  $\delta$  8.49–8.26 (m, 1H), 8.19 (d,  $J = 8.5$  Hz, 2H), 8.17–7.98 (m, 1H), 7.64 (d,  $J = 8.5$  Hz, 1H), 7.58–7.45 (m, 2H), 7.28 (d,  $J = 8.0$  Hz, 1H), 6.93 (d,  $J = 8.5$  Hz, 2H), 3.06 (s, 6H).  $^{13}\text{C}$  NMR (101 MHz,  $\text{CDCl}_3$ )  $\delta$  149.99, 136.30, 127.88, 124.75, 124.01, 123.88, 122.85, 120.84, 119.79, 119.51, 115.65, 112.52, 111.44, 40.41. HRMS (ESI-Q-TOF):  $m/z$   $[\text{M}]$  calcd for  $\text{C}_{20}\text{H}_{16}\text{ClN}_5$ : 361.1094, found: 361.1090.

#### 4. Conclusions

In summary, novel heteroaryl-fused triazapentalene derivatives were developed by Suzuki cross-coupling and palladium-catalyzed arylation reactions. The yields of Suzuki cross-coupling reactions were not satisfactory, while the direct CH arylation reaction was justified to be an effective strategy. In terms of photophysical properties, **HetATAP1-5** are virtually non-luminescent in the solution state, but exhibit luminescent behavior in the solid-state and possess AIEE properties upon aggregation. Furthermore, substituents with electronic groups do not affect the fluorescence properties in solution, whereas they are slightly affected in the solid-state. In particular, compounds **HetATAP3** and **HetATAP4** were studied for their AIEE properties in ACN/water and THF/water (10:0 to 1:9), respectively. It was also observed that in these mixtures, solvent system and duration affect the AIEE photoluminescence of **HetATAP3** and **HetATAP4**. In particular, the AIEE fluorescence color of these HetATAPs can be tuned by introducing different substituents on the indazole ring.

**Supplementary Materials:** The following supporting information can be downloaded at the website of this paper posted on Preprints.org.

**Author Contributions:** Conceptualization, Y.W. and W.D.; methodology, Y.W.; validation, Y.W. and J.W.; investigation, Y.W.; writing—original draft preparation, Y.W. and J. W; writing—review and editing, Y.W. and W.D.; supervision, W.D.; funding acquisition, W.D. All authors have read and agreed to the published version of the manuscript.

**Funding:** This research was funded by the Research Council of KU Leuven through projects C14/19/78 and C14/19/079 (FUEPONA). Y.W. received a doctoral fellowship from the China Scholarship Council (201706920044) and the research fellowship from Henan University of Urban Construction (990/K-Q2024015). Mass spectrometry was made possible by the support of the Hercules Foundation of the Flemish Government (20100225-7) and NMR spectroscopy by Hercules grants I002720N and G0D6221N. The purchase of the diffractometer was supported by the Hercules Foundation through project AKUL/09/0035.

**Data Availability Statement:** The original contributions presented in the study are included in the article/Supplementary Material; further inquiries can be directed to the corresponding authors.

**Acknowledgments:** The authors acknowledge Bart Van Huffel for technical assistance with the NMR spectrometers, and Jef Rozenski for the HRMS measurements.

**Conflicts of Interest:** The authors declare no conflicts of interest.

#### References



1. Wang Y, Opsomer T, Dehaen W. Developments in the chemistry of 1,3a,6a-triazapentalenes and their fused analogs [Internet]. 1st ed. Vol. 137, *Advances in Heterocyclic Chemistry*. Elsevier Inc.; 2022. 25–70 p. Available from: <http://dx.doi.org/10.1016/bs.aihch.2021.10.002>
2. Nyffenegger C, Pasquinet E, Suzenet F, Poullain D, Guillaumet G. Synthesis of nitro-functionalized polynitrogen tricycles bearing a central 1,2,3-triazolium ylide. *Synlett*. 2009;3(8):1318–20.
3. Nyffenegger C, Pasquinet E, Suzenet F, Poullain D, Jarry C, Léger JM, et al. An efficient route to polynitrogen-fused tricycles via a nitrene-mediated N-N bond formation under microwave irradiation. *Tetrahedron*. 2008;64(40):9567–73.
4. González J, Santamaría J, Suárez-Sobrinho ÁL, Ballesteros A. One-Pot and Regioselective Gold-Catalyzed Synthesis of 2-Imidazolyl-1-pyrazolylbenzenes from 1-Propargyl-1H-benzotriazoles, Alkynes and Nitriles through  $\alpha$ -Imino Gold(I) Carbene Complexes. *Adv Synth Catal*. 2016;358(9):1398–403.
5. Legentil P, Chadeyron G, Therias S, Chopin N, Sirbu D, Suzenet F, et al. Luminescent N-heterocycles based molecular backbone interleaved within LDH host structure and dispersed into polymer. *Appl Clay Sci* [Internet]. 2020;189(March):105561. Available from: <https://doi.org/10.1016/j.clay.2020.105561>
6. Daniel M, Hiebel MA, Guillaumet G, Pasquinet E, Suzenet F. Intramolecular Metal-Free N–N Bond Formation with Heteroaromatic Amines: Mild Access to Fused-Triazapentalene Derivatives. *Chem - A Eur J*. 2020;26(7):1525–9.
7. Sirbu D, Diharce J, Martinić I, Chopin N, Eliseeva S V., Guillaumet G, et al. An original class of small sized molecules as versatile fluorescent probes for cellular imaging. *Chem Commun*. 2019;55(54):7776–9.
8. Katritzky AR, Hür D, Kirichenko K, Ji Y, Steel PJ. Synthesis of 2, 4-disubstituted furans and 4, 6-diaryl-substituted 2, 3-benzo-1, 3a, 6a-triazapentalenes. *Arkivoc*. 2004;2:109–21.
9. VOI N, Lynch BM, Hung YY. Pyrazolo [ 1,2-a] benzotriazole and Related Compounds (1). *J Heterocycl Chem*. 1965;2(1):218–9.
10. Albini A, Bettinetti G, Minoli G. The effect of the p-nitro group on the chemistry of phenylnitrene. A study via intramolecular trapping. *J Chem Soc Perkin Trans 2*. 1999;(12):2803–7.
11. Albini BA, Bettinetti GF, Minoli G, Pietra S. Singlet Oxygen Photo-oxidation of some Triazapentalenes By. *J Chem Soc Perkin Trans 1*. 1980;0(2904):2–6.
12. Sirbu D, Diharce J, Martinić I, Chopin N, Eliseeva S V, Guillaumet G, et al. An original class of small sized molecules as versatile fluorescent probes for cellular imaging. *Chem Commun* [Internet]. 2019;55(54):7776–9. Available from: <http://dx.doi.org/10.1039/C9CC03765A>
13. Luo J, Xie Z, Xie Z, Lam JWY, Cheng L, Chen H, et al. Aggregation-induced emission of 1-methyl-1,2,3,4,5-pentaphenylsilole. *Chem Commun*. 2001;18:1740–1.
14. Lian X, Sun J, Zhan Y. Dibenzthiophene and carbazole modified dicyanoethylene derivative exhibiting aggregation-induced emission enhancement and mechanochromic luminescence. *J Lumin*. 2023;263:120023.
15. Zhuang Q, Zeng C, Mu Y, Zhang T, Yi G, Wang Y. Lead (II)-triggered aggregation-induced emission enhancement of adenosine-stabilized gold nanoclusters for enhancing photoluminescence detection of nabam—disodium ethylenebis (dithiocarbamate). *Chem Eng J*. 2023;470:144113.
16. Liu D, Guo X, Wu H, Chen X. Aggregation-induced emission enhancement of gold nanoclusters triggered by sodium heparin and its application in the detection of sodium heparin and alkaline amino acids. *Spectrochim Acta Part A Mol Biomol Spectrosc*. 2024;304:123255.
17. An Y, Li B, Yu Y, Zhou Y, Yi J, Li L, et al. A rapid and specific fluorescent probe based on aggregation-induced emission enhancement for mercury ion detection in living systems. *J Hazard Mater*. 2024;465:133331.
18. Nelson M, Santhalingam G, Ashokkumar B, Ayyanar S, Selvaraj M. Aggregation induced emission enhancement (AIEE) receptor for the rapid detection of Cu<sup>2+</sup> ions with in vivo studies in A549 and AGS gastric cancer cells. *Microchem J*. 2023;194:109294.
19. Nurnabi M, Gurusamy S, Wu JY, Lee CC, Sathiyendiran M, Huang SM, et al. Aggregation-induced emission enhancement (AIEE) of tetrarhenium (I) metallacycles and their application as luminescent sensors for nitroaromatics and antibiotics. *Dalt Trans*. 2023;52(7):1939–49.
20. Chen G, Wang J, Chen W, Gong Y, Zhuang N, Liang H, et al. Triphenylamine-functionalized multiple-resonance TADF emitters with accelerated reverse intersystem crossing and aggregation-induced emission enhancement for narrowband OLEDs. *Adv Funct Mater*. 2023;33(12):2211893.
21. Arshad M, AT JR, Joseph V, Joseph A. Selective detection of picric acid in aqueous medium using a novel naphthaldehyde-based aggregation induced emission enhancement (AIEE) active “turn-off” fluorescent sensor. *J Lumin*. 2023;258:119818.
22. Turelli M, Ciofini I, Wang Q, Ottochian A, Labat F, Adamo C. Organic compounds for solid state luminescence enhancement/aggregation induced emission: a theoretical perspective. *Phys Chem Chem Phys*. 2023;25(27):17769–86.
23. Li S, Zhang H, Huang Z, Jia Q. Fluorometric and colorimetric dual-mode sensing of  $\alpha$ -glucosidase based on aggregation-induced emission enhancement of AuNCs. *J Mater Chem B*. 2024;12(6):1550–7.



24. Yin S, Peng Q, Shuai Z, Fang W, Wang Y hua, Luo Y. Aggregation-enhanced luminescence and vibronic coupling of silole molecules from first principles. *Phys Rev B* [Internet]. 2006;73:205409. Available from: <https://api.semanticscholar.org/CorpusID:121544093>
25. Liu J, Lam JWY, Tang BZ. Aggregation-induced Emission of Silole Molecules and Polymers: Fundamental and Applications. *J Inorg Organomet Polym Mater* [Internet]. 2009;19(3):249–85. Available from: <https://doi.org/10.1007/s10904-009-9282-8>
26. Zhao Z, He B, Tang BZ. Aggregation-induced emission of siloles. *Chem Sci*. 2015;6(10):5347–65.
27. Wang Z, Gu Y, Liu J, Cheng X, Sun JZ, Qin A, et al. A novel pyridinium modified tetraphenylethene: AIE-activity, mechanochromism, DNA detection and mitochondrial imaging. *J Mater Chem B*. 2018;6(8):1279–85.
28. Dong Y, Lam JWY, Qin A, Liu J, Li Z, Tang BZ, et al. Aggregation-induced emissions of tetraphenylethene derivatives and their utilities as chemical vapor sensors and in organic light-emitting diodes. *Appl Phys Lett*. 2007;91(1).
29. Ito F, Fujimori J ichi, Oka N, Sliwa M, Ruckebusch C, Ito S, et al. AIE phenomena of a cyanostilbene derivative as a probe of molecular assembly processes. *Faraday Discuss*. 2017;196:231–43.
30. Ito F, Fujimori J ichi, Oka N, Sliwa M, Ruckebusch C, Ito S, et al. AIE phenomena of a cyanostilbene derivative as a probe of molecular assembly processes. *Faraday Discuss*. 2016 Nov 30;196.
31. Bhongale CJ, Chang CW, Lee CS, Diao EWG, Hsu CS. Relaxation dynamics and structural characterization of organic nanoparticles with enhanced emission. *J Phys Chem B*. 2005;109(28):13472–82.
32. Itami K, Ohashi Y, Yoshida JI. Triarylethene-based extended  $\pi$ -systems: Programmable synthesis and photophysical properties. *J Org Chem*. 2005;70(7):2778–92.
33. Ziótek M, Filipczak K, Maciejewski A. Spectroscopic and photophysical properties of salicylaldehyde azine (SAA) as a photochromic Schiff base suitable for heterogeneous studies. *Chem Phys Lett*. 2008;464(4–6):181–6.
34. Arcovito G, Bonamico M, Domenicano A, Vaciago A. Crystal and molecular structure of salicylaldehyde azine. *J Chem Soc B Phys Org*. 1969;733–41.
35. Sirbu D, Chopin N, Martinić I, Ndiaye M, Eliseeva S V., Hiebel MA, et al. Pyridazino-1,3a,6a-triazapentalenes as versatile fluorescent probes: Impact of their post-functionalization and application for cellular imaging. *Int J Mol Sci*. 2021;22(12):1–10.
36. Wang Y, Opsomer T, de Jong F, Verhaeghe D, Mulier M, Van Meervelt L, et al. Palladium-Catalyzed Arylations towards 3,6-Diaryl-1,3a,6a-triazapentalenes and Evaluation of Their Fluorescence Properties. *Molecules*. 2024;29(10).
37. Gorelsky SI, Lapointe D, Fagnou K. Analysis of the concerted metalation-deprotonation mechanism in palladium-catalyzed direct arylation across a broad range of aromatic substrates. *J Am Chem Soc*. 2008;130(33):10848–9.
38. Zheng J, Huang F, Li Y, Xu T, Xu H, Jia J, et al. The aggregation-induced emission enhancement properties of BF<sub>2</sub> complex isatin-phenylhydrazone: Synthesis and fluorescence characteristics. *Dye Pigment*. 2015;113:502–9.
39. Turchini GM, Ng WK, Tocher DR. Fish oil replacement and alternative lipid sources in aquaculture feeds. CRC Press; 2010.
40. Zhang Y, Qi X, Cui X, Shi F, Deng Y. Palladium catalyzed N-alkylation of amines with alcohols. *Tetrahedron Lett*. 2011;52(12):1334–8.

**Disclaimer/Publisher's Note:** The statements, opinions and data contained in all publications are solely those of the individual author(s) and contributor(s) and not of MDPI and/or the editor(s). MDPI and/or the editor(s) disclaim responsibility for any injury to people or property resulting from any ideas, methods, instructions or products referred to in the content.